DYNAMIC ANALYSIS OF THE LOAD HOISTING PROCESS

JULIUSZ GRABSKI
JAROSŁAW STRZAŁKO

Faculty of Mechanical Engineering, Technical University of Łódź

e-mail: julgrabs@p.lodz.pl

Proposals of two models of a load lifted by cranes have been discussed. Special attention has been paid to the phenomena occurring before detachment of the load from the ground. Stick-slip motion of the load on the foundation has been observed. One of two models presented – the model in the form of a rigid body resting on an elastic foundation has turned out to be more advantageous for the analysis of the lifting process. The results of numerical computations have revealed a phenomenon of solution bifurcation that occurs at a slight change in values of parameters of the model.

Key words: cranes, 3D model of load, dynamics of lifted load, load hoisting

1. Introduction

The load hoisting process is an interesting problem in dynamics of bodies. The positioning of a load and anti-sway prevention are examples of practical applications.

The task that consists in computer simulation of load motion during its lifting from the ground in the situation when the rope direction is not vertical can be of significance from the practical point of view. Under normal operating conditions of a crane, this way of lifting a load is not proper, however it can take place under certain circumstances. For instance, for rescue trucks equipped with cranes that are used to lift auto hulks out of ditches, this kind of work is not exceptionally rare.

When there is a necessity to shift a load with respect to the ground or if the vertical direction of the rope cannot be maintained, the lifting process

becomes complex. In such cases, frictional effects, rotations of the load, and load impacts due to collisions with the ground may occur. The consideration of these phenomena makes the algorithm and the load dynamics analysis more complex. Thus, a rigid body seems to be a suitable load model for such a task (cf. Strzałko and Grabski, 1998).

In the literature devoted to lifting and carrying loads, the most often model of the lifted load is a particle (e.g. Borkowski *et al.*, 1996, Jedliński and Grzesikiewicz, 1990; Strzałko and Grabski, 1995; Hakala and Sorsa, 1998; Maczyński and Kościelny, 1999; Tomczyk and Cink, 1999; Miyata *et al.*, 2001; etc.), and sometimes a 2D rigid body (cf. Grabski 1998). A three-dimensional model of a crane and a particle model of a load has been analysed by Wojnarowski *et al.* (1990), Lee (1998). In the papers by Grabski and Strzałko (1997), Grabski (1998), Strzałko (1998), a 3D body was the model of the lifted load, and in those cases mechanical parameters (e.g. rotation inertia of the body, positions of the body mass centre and the rope fixture) of the lifted load could be considered.

In the present study, two models of the load have been compared. They differ as far as the body-ground contact modelling is concerned. In the first case, a direct contact between the rigid body and the rigid foundation has been assumed. In the second case, it has been assumed that the rigid body contacts the elastic foundation.

Linearly elastic models of bodies, which are employed in contact problems (e.g. Konderla, 1993; Wriggers and Zavarise, 1993), describe well local phenomena in the contact region of flexible solids. These phenomena can serve as a clue for the distribution of surface forces (ground reactions) acting on the load. In the analysis of load motion, especially finite motions, the determination of local deformations of the body and the foundation is not important.

The relationships presented in this paper, which describe the initial period of the crane operation, i.e. rope tensioning, stick-slip motion of the load with respect to the ground, the moment of detachment and motion of the load after its detachment, concern systems in which the lifted load is modelled as a 3D rigid body. In the problem solutions known to the authors, these issues are usually neglected.

The results of numerical calculations prove quantitative and qualitative agreement between the results obtained for both the models. However, in the analysis of the lifting process, the model of the load in the form a rigid body resting on an elastic foundation is more suitable. The application of this model leads to a simpler and more effective calculation algorithm, which results from a constant number of degrees of freedom in the system during the whole process

of analysis. The model in which a rigid body contacts a rigid foundation is characterised by a time-varying number of degrees of freedom of the load that depends on the motion phase (the number of degrees of freedom during shifting the load with respect to the ground is different from the number of degrees of freedom during rotation of the load with respect to the edge or the corner, and it is still different at the moment when there is no contact with the ground).

An interesting phenomenon that occurred during the numerical computations is bifurcation of the solution. The model of the load under consideration is a non-linear multidimensional system with dry friction. For systems of this sort, a slight change in the value of one parameter can result in bifurcation of the solution in some ranges of values of parameters (cf. Kurnik, 1997). Friction coefficient value between the load and the ground has been chosen as an active (bifurcation) parameter. The results presented in this paper illustrate evolution of the solution at a slight change in the bifurcation parameter.

2. First model – a rigid body on a rigid foundation

The first model to be considered is a rigid body placed on an ideally rigid foundation.
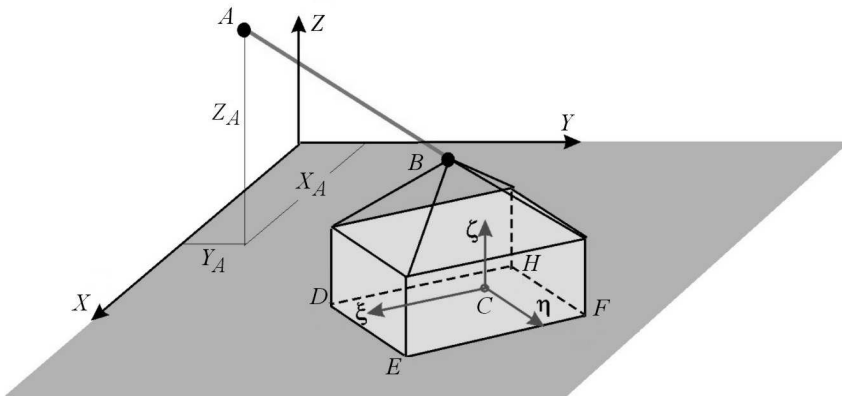
Fig. 1. Model of the load – characteristic points, systems of co-ordinates

Reaction forces between the ground and the rigid body can be presented in various manners. In Fig. 2, the normal components of the foundation reaction have been presented separately, and the friction forces are presented aside.
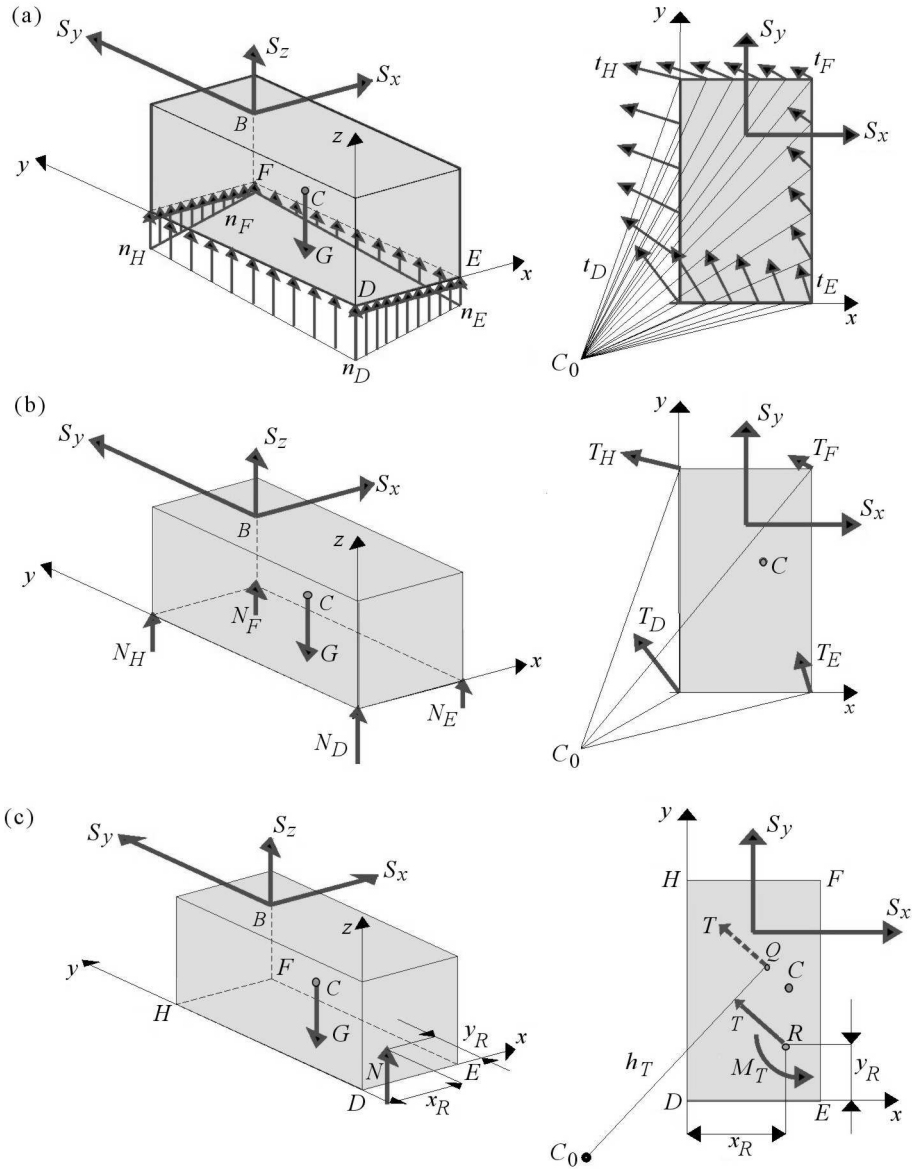
Fig. 2. Equivalent free-body diagrams of the load: (a) on the assumption of a continuous distribution of the reaction forces; (b) for forces concentrated in corners; (c) in the case of the reduced loading

A distribution of the foundation reaction components is presented for the following cases, subsequently:

a) normal forces $\boldsymbol{n}(x, y)$ and tangent forces $\boldsymbol{t}(x, y)$ distributed on the surface in a continuous way (in Fig. 2a a distribution of these forces along the body edge is shown only);

b) concentrated forces $(\boldsymbol{N}_D, \boldsymbol{T}_D, \boldsymbol{N}_E, \boldsymbol{T}_E, \boldsymbol{N}_F, \boldsymbol{T}_F, \boldsymbol{N}_H, \boldsymbol{T}_H)$ applied to the body corners (Fig. 2b);

c) reduced concentrated loading acting in a given point R of the surface of the contact between bodies (the tangent force $\boldsymbol{T}$ and the normal reaction force $\boldsymbol{N}$) and the couple ($\boldsymbol{T}$ and $-\boldsymbol{T}$) with the moment value denoted by M_T (Fig. 2c).

2.1. Analysis of the equilibrium of the load

The presented ways of an introduction force reaction of the ground are equivalent statically, if the following is assumed:

– for the model with distributed forces (Fig. 2a) – a linear change in the values of normal reaction forces with respect to the ground, i.e.

$$n(x, y) = a_0 + a_1 x + a_2 y \qquad (2.1)$$

(xyz is the body local co-ordinate system) and the corresponding values of tangent forces

$$t(x, y) \leqslant \mu n(x, y) \qquad (2.2)$$

– for the model with forces concentrated in corners (Fig. 2b) – a linear relationship that describes the values of normal reactions components

$$N_i(x_i, y_i) = A_0 + A_1 x_i + A_2 y_i \qquad i = D, E, F, H \qquad (2.3)$$

and the friction forces applied in the same points, whose values satisfy the following conditions

$$T_i \leqslant \mu N_i \qquad i = D, E, F, H \qquad (2.4)$$

– for the model in the form of the resultant forces $\boldsymbol{T}$ and $\boldsymbol{N}$ (Fig. 2c) and the moment $\boldsymbol{M}_T$ that follows from the reduction of friction forces to the point R

$$T \leqslant \mu N \qquad (2.5)$$

The directions and senses of the friction forces are defined by the directions of possible velocities.

The following relations hold

$$N = N_D + N_E + N_F + N_H = \int\limits_0^a \int\limits_0^b n(x,y)\,dxdy$$

$$T_x = T_{Dx} + T_{Ex} + T_{Fx} + T_{Hx} = \int\limits_0^a \int\limits_0^b t_x(x,y)\,dxdy$$

$$T_y = T_{Dy} + T_{Ey} + T_{Fy} + T_{Hy} = \int\limits_0^a \int\limits_0^b t_y(x,y)\,dxdy \qquad (2.6)$$

$$T = \sqrt{T_x^2 + T_y^2}$$

$$M_T = T_{Dx}y_R - T_{Dy}x_R + T_{Ex}y_R + T_{Ey}(x_E - x_R) - T_{Fx}(y_F - y_R) +$$

$$+ T_{Fy}(x_F - x_R) - T_{Hx}(y_H - y_R) - T_{Hy}x_R =$$

$$= \int\limits_0^a \int\limits_0^b [t_x(y - y_R) + t_y(x - x_R)]\,dxdy$$

The forces distributed continuously are described by the quantities n_D, n_E, n_F and n_H, which denote the values of pressure per unit area in individual corners. An exemplary relation describing n_D has the following form

$$n_D = \frac{7ab(G - S_z) + 6b(S_z x_B - G x_C - S_x z_B) + 6a(S_z y_B - G y_C - S_y z_B)}{a^2 b^2}$$

$$(2.7)$$

The values of forces concentrated in corners (N_E, N_F and N_H) can be determined from formulas similar to that one for N_D

$$N_D = \frac{3ab(G - S_z) + 2b(S_z x_B - G x_C - S_x z_B) + 2a(S_z y_B - G y_C - S_y z_B)}{4ab}$$

$$(2.8)$$

On the basis of the equations of equilibrium, the co-ordinates (x_R, y_R) of the point R, through which the resultant reaction force $N = G - S_z$ comes through, and the values of the friction force $T = \sqrt{S_x^2 + S_y^2}$ as well as their moment M_T can be determined.

During the analysis of the system, the state of equilibrium is controlled. The system under analysis is in the state of equilibrium for

$$N > 0 \qquad\qquad T < \mu N$$

$$|M_T| < \max_i |T_x(y_i - y_R) - T_y(x_i - x_R)| \qquad i = D, E, F, H \quad (2.9)$$

$$0 < x_R < a \qquad\qquad 0 < y_R < b$$

If the above-mentioned conditions of the equilibrium are not satisfied, a transition to the next calculation phase takes place, namely to solving the equations of motion of the model under analysis.

2.2. Equations of motion of the system

The motion of the body is analysed by means of the Newton-Euler equations that describe general motion of the body (displacements of the mass center and rotations)

$$m\boldsymbol{p}_C = \sum \boldsymbol{P} \qquad\qquad \frac{\check{d}\boldsymbol{K}_C}{dt} + \boldsymbol{\omega} \times \boldsymbol{K}_C = \sum \boldsymbol{M}_C \qquad (2.10)$$

These equations in the matrix form are presented as follows

$$
m\begin{bmatrix} \ddot{X}_C \\ \ddot{Y}_C \\ \ddot{Z}_C \end{bmatrix} = \begin{bmatrix} S_X \\ S_Y \\ S_Z \end{bmatrix} + \begin{bmatrix} T_X \\ T_Y \\ N - G \end{bmatrix}
$$

$$
\begin{bmatrix} J_\xi & -J_{\xi\eta} & -J_{\xi\zeta} \\ -J_{\xi\eta} & J_\eta & -J_{\eta\zeta} \\ -J_{\xi\zeta} & -J_{\eta\zeta} & J_\zeta \end{bmatrix} \begin{bmatrix} \dot{\omega}_\xi \\ \dot{\omega}_\eta \\ \dot{\omega}_\zeta \end{bmatrix} + \begin{bmatrix} 0 & -\omega_\zeta & \omega_\eta \\ \omega_\zeta & 0 & -\omega_\xi \\ -\omega_\eta & \omega_\xi & 0 \end{bmatrix} \cdot
$$

$$
\cdot \begin{bmatrix} J_\xi & -J_{\xi\eta} & -J_{\xi\zeta} \\ -J_{\xi\eta} & J_\eta & -J_{\eta\zeta} \\ -J_{\xi\zeta} & -J_{\eta\zeta} & -J_\zeta \end{bmatrix} \begin{bmatrix} \omega_\xi \\ \omega_\eta \\ \omega_\zeta \end{bmatrix} = \begin{bmatrix} 0 & -\zeta_B & \eta_B \\ \zeta_B & 0 & -\xi_B \\ -\eta_B & \xi_B & 0 \end{bmatrix} \begin{bmatrix} S_\xi \\ S_\eta \\ S_\zeta \end{bmatrix} +
$$

$$
+ \begin{bmatrix} 0 & -\zeta_Q & \eta_Q \\ \zeta_Q & 0 & -\xi_Q \\ -\eta_Q & \xi_Q & 0 \end{bmatrix} \begin{bmatrix} T_\xi \\ T_\eta \\ T_\zeta \end{bmatrix} + \begin{bmatrix} 0 & -\zeta_R & \eta_R \\ \zeta_R & 0 & -\xi_R \\ -\eta_R & \xi_R & 0 \end{bmatrix} \begin{bmatrix} N_\xi \\ N_\eta \\ N_\zeta \end{bmatrix}
$$

$$(2.11)$$

where $\ddot{X}_C$, $\ddot{Y}_C$, $\ddot{Z}_C$ denote the projections of the acceleration vector of the point C on the axes of the fixed coordinate system (XYZ), $\dot{\omega}_\xi$, $\dot{\omega}_\eta$, $\dot{\omega}_\zeta$ are the projections of the angular acceleration vector of the body on the axes attacheed to the body $(\xi\eta\zeta)$, whereas (ξ_B, η_B, ζ_B), (ξ_R, η_R, ζ_R), (ξ_Q, η_Q, ζ_Q)

are the co-ordinates that describe the positions of B, R and Q in which the forces $\boldsymbol{S}$, $\boldsymbol{N}$ and $\boldsymbol{T}$ are applied, respectively.

The motion of the boom tip (modelled with a particle of the mass m_0, which is located at the end of the boom) is described by the following vector equation

$$m_0 \boldsymbol{p}_A = \sum \boldsymbol{P}_0 \qquad (2.12)$$

It means

$$m_0 \begin{bmatrix} \ddot{X}_A \\ \ddot{Y}_A \\ \ddot{Z}_A \end{bmatrix} = \begin{bmatrix} k_X \Delta X_A \\ k_Y \Delta Y_A \\ k_Z \Delta Z_A \end{bmatrix} + \begin{bmatrix} -S_X \\ -S_Y \\ -(S_Z + G_0) \end{bmatrix} \qquad (2.13)$$

where: k_X, k_Y, k_Z denote the equivalent stiffnesses of the boom, and ΔX_A, ΔY_A, ΔZ_A – its deformations.

Two additional equations are used in the mathematical model. In the case of an elastic rope, the rope tension is obtained as

$$S = c_l \left[\sqrt{(X_B - X_A)^2 + (Y_B - Y_A)^2 + (Z_B - Z_A)^2} - l(t) \right] \qquad (2.14)$$

where c_l is the rope stiffness and $l(t)$ the rope length. For the model of an inextensible rope, the geometrical constraint equation is introduced

$$(X_B - X_A)^2 + (Y_B - Y_A)^2 + (Z_B - Z_A)^2 - [l(t)]^2 = 0 \qquad (2.15)$$

The number of degrees of freedom and the form of the equations of motion of the load undergo changes during the lifting process. Both the number of relations that describe constraints and the form of constraint equations change. The subsequent phases of motion are solved with procedures including proper relations for each phase.

The conditions and equations describing one phase of motion will be shown by means of an example of the sliding of the load on the ground.

2.3. The sliding of the load

If the following conditions are fulfilled

$$Z_i = 0 \qquad i = D, E, F, H$$

$$T = \mu N \quad N > 0 \qquad \begin{aligned} 0 < x_R < a \\ 0 < y_R < b \end{aligned} \qquad (2.16)$$

the body slides along the ground – plane motion of the body occurs.

The equations of motion are obtained on the basis of relations (2.11), after the following substitutions: $\omega_\zeta = \dot\psi$, $\ddot Z_C = 0$, $\omega_\xi = 0$, $\omega_\eta = 0$, $\dot\omega_\xi = 0$, $\dot\omega_\eta = 0$, $\vartheta = 0$, $\varphi = 0$, (and also: $N_\eta = N_\xi = 0$, $N_\zeta = N$, $T_\zeta = 0$).

The resulting system of algebraic and differential equations should be supplemented with additional kinematics relationships which define the constraints imposed on the directions of friction forces

$$
\begin{aligned}
V_{i\xi} &= \dot X_C \cos\psi + \dot Y_C \sin\psi + \dot\psi\eta_i & i &= D, E, F, H \\
V_{i\eta} &= \dot Y_C \cos\psi - \dot X_C \sin\psi + \dot\psi\xi_i & i &= D, E, F, H
\end{aligned}
\tag{2.17}
$$

The components of friction forces, applied in individual corners, are determined then as

$$
\begin{aligned}
T_{i\xi} &= -\mu N_i \frac{V_{i\xi}}{\sqrt{V_{i\xi}^2 + V_{i\xi}^2}} & i &= D, E, F, H \\
T_{i\eta} &= -\mu N_i \frac{V_{i\eta}}{\sqrt{V_{i\eta}^2 + V_{i\eta}^2}} & i &= D, E, F, H
\end{aligned}
\tag{2.18}
$$

and their sum, according to $(2.6)_{2,3}$, yields the resultant friction force components T_ξ, T_η. The coordinates of the point Q, where the resultant friction force is applied, can be described by means of the following relations, thus

$$
\begin{aligned}
\xi_Q &= \frac{1}{T_\eta}(T_{\eta D}\xi_D + T_{\eta E}\xi_E + T_{\eta F}\xi_F + T_{\eta H}\xi_H) \\
\eta_Q &= \frac{1}{T_\xi}(T_{\xi D}\eta_D + T_{\xi E}\eta_E + T_{\xi F}\eta_F + T_{\xi H}\eta_H) \\
\zeta_Q &= -Z_C
\end{aligned}
\tag{2.19}
$$

The derived equations allow for determination of the quantities being sought: $X_C(t)$, $Y_C(t)$, $\psi(t)$ and $N(t)$, $T_\xi(t)$, $T_\eta(t)$, $\xi_N(t)$, $\eta_N(t)$, $\xi_Q(t)$, $\eta_Q(t)$ during the load sliding on the ground.

An example of the solution, in which the quoted relations are used, is shown in Fig. 3. The motion of the load is forced by a change in the rope length $l(t) = l_0 - v_l t$. The calculations have been carried out for the following data:

- load dimensions: $a = 2.5\,\mathrm{m}$, $b = 6.0\,\mathrm{m}$, $c = 2.5\,\mathrm{m}$
- co-ordinates of the point A of the rope $\mathbf{x}_A = [3.0, 4.0, 10.0]$
- load density $\rho = 1000\,\mathrm{kg/m}^3$
- coefficient of friction between the load and the ground $\mu = 0.25$.
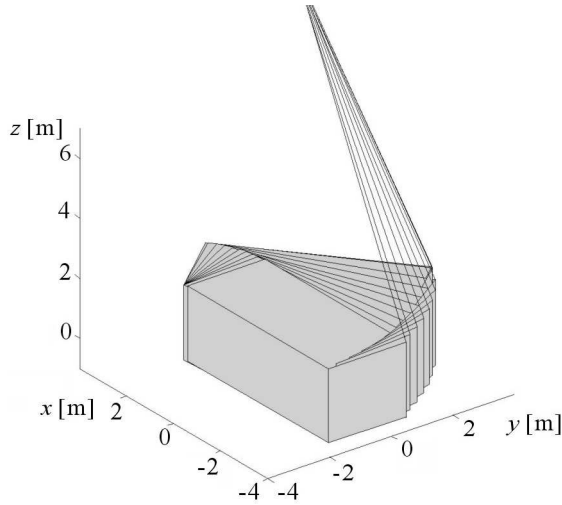
Fig. 3. Results of simulation of the load sliding

The placing of the connection point of the rope and container in the container corner causes that the load slides along the ground in the first phase of motion.

In the case when conditions (2.16) are not satisfied, and thus motion of the load is not plane, other solution paths are foreseen in the algorithm. A choice of the solution path is made automatically.

3.   Second model – a rigid body on an elastic foundation

The second model under consideration is a rigid body that contacts an elastic foundation. This contact is made by elastic and damping elements, whose directions remain vertical (parallel to the axis Z), Fig. 4.

It is assumed that the reaction forces of the ground are in this case concentrated forces applied to the corners of the body N_D, T_D, N_E, T_E, N_F, T_F, N_H, T_H. For negative vertical displacements of the corners $Z_i < Z_0$, the normal forces N_D, N_E, N_F, N_H are assumed according to the relation

$$N_i(x_i, y_i) = kZ_i + h\dot{Z}_i \qquad\qquad i = D, E, F, H \qquad\qquad (3.1)$$
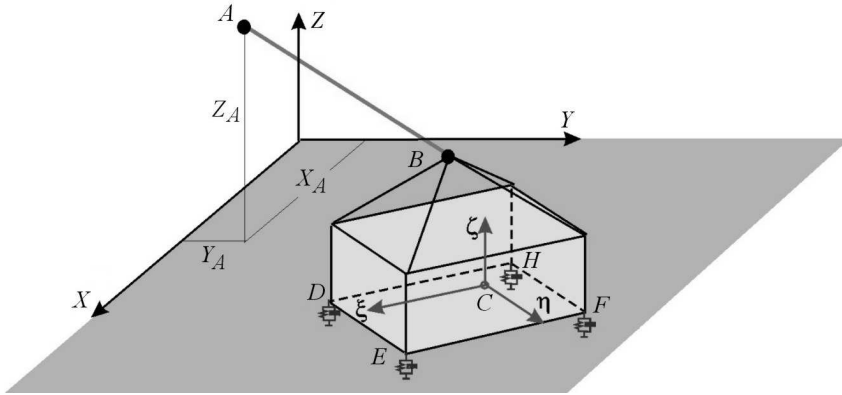
Fig. 4. Model of the load placed on the elastic foundation

whereas for positive distances of the corners from the foundation surface $Z_i > Z_0$, zero normal forces are assumed

$$N_i(x_i, y_i) = 0 \qquad i = D, E, F, H \qquad (3.2)$$

The symbol k denotes the stiffness of the elastic elements introduced, h refers to the coefficient of damping of the damping elements. The values of both the coefficients are selected by means of a numerical experiment.

The friction forces acting in the corners of the body have the values

$$T_i = \mu N_i \qquad i = D, E, F, H \qquad (3.3)$$

whereas their directions are determined by the corner velocity directions[1].

3.1. Analysis of the equilibrium of the load

The model equipped with springs and damping elements remains in the equilibrium only in the case when the force the rope acts with is equal to zero. The friction forces are equal to zero under such a loading. An increase in the loading caused by the rope results in small displacements of the system and in an appearance of frictional effects.

The state in which the load rests on the ground – for a non-zero loading generated by the rope – cannot be realised in such a model. When a loading

---

[1]The zero corner vertical velocity, which means $T_i < \mu N_i$ ($i = D, E, F, H$), violates the calculation procedure, as the number of degrees of freedom of the system changes in this case. The procedure indicates this situation. In the calculations carried out, such an instance did not occur.

occurs, small displacements occur as well. A proper selection of the coeffi-
cients of elasticity and damping of the foundation allows for reducing these
displacements to magnitudes that are insignificant from the practical point of
view.

3.2. Motion analysis

The application of the load model in the form of a rigid body placed on an
elastic foundation allows the avoiding of the necessity of analysing the system
with a time-varying number of degrees of freedom. Instead of the limitations
imposed by analytically described constraints on the relations between certain
co-ordinates, some limitations in the form of reaction forces of the ground have
been introduced. It turns out that the selection of these forces is rather simple.
Such an approach simplifies considerably the process of numerical solution of
the load motion issue. The number of degrees of freedom of the system and
the form of equations do not change during the problem solving.

The equations of motion of the model under discussion have been generated
by computer. Lagrange's equations of the second kind have been employed
for this purpose. The assumed method requires only determination of the
kinetic energy of the system, the generalised forces acting on the system and
the initial conditions. The remaining procedures are made by computer. The
kinetic energy of the system under analysis is described by the formula

$$T = \frac{1}{2}\dot{\mathbf{q}}_1^\top \mathbf{M}\dot{\mathbf{q}}_1 + \dot{\mathbf{q}}_2^\top \mathbf{R}_1^\top \mathbf{J}\mathbf{R}_1\dot{\mathbf{q}}_2 + \frac{1}{2}\dot{\mathbf{q}}_1^\top \mathbf{R}^\top \mathbf{M}\mathbf{W}\mathbf{R}_1\dot{\mathbf{q}}_2 \qquad (3.4)$$

where: $\mathbf{q}_1 = [X_C, Y_C, Z_C]^\top$ and $\mathbf{q}_2 = [\varphi, \psi, \vartheta]^\top$ denote the generalised co-
ordinates of the load; $\mathbf{M}$, $\mathbf{J}$ are the matrices of masses and moments of inertia
of the load; $\mathbf{R}_1$, $\mathbf{R}$ stand for the matrices of transformations of the co-ordinates;
$\mathbf{W}$ refers to the antisymmetric matrix of the co-ordinates of the mass centre
of the load (of the point C) in the body co-ordinate system $\xi\eta\zeta$.

4.   Calculation results and conclusions

The *Mathematica* and *Matlab* software packages were used in the analysis
and calculations carried out for the models of the load under consideration.
The *Mathematica* was used to generate the equations of motion, whereas the
numerical calculations were conducted with the *Matlab*.

The results of the calculations allow for drawing a few conclusions.

4.1. Comparison of the results for different models of the system

In Fig. 5 and Fig. 6 the results of calculations for both load models are presented, i.e.: a rigid body placed on an ideally rigid foundation and a body placed on an elastic foundation. The plots include time histories of the co-ordinates describing the location of the mass centre of the load (Fig. 5) and the reaction forces from the ground at the contact point with the body (Fig. 6a) and the force acting in the rope (Fig. 6b). The obtained results for both models are slightly different.

The calculations were carried out for the following data:

– container dimensions: $a = 2.5$ m, $b = 6.0$ m, $c = 2.5$ m

– mean density of the container material $\rho = 1000.0$ kg/m^3

– properties of the foundation: coefficient of friction 0.15, coefficient of elasticity $k = 1.5 \cdot 10^7$ N/m, coefficient of viscous damping $h = 0.2 \cdot 10^6$ Ns/m – in the case of the elastic foundation model

– properties of the rope: coefficient of elasticity $c_l = 1.5 \cdot 10^7$ N/m, coefficient of viscous damping $b_l = 1.3 \cdot 10^4$ Ns/m

– hoisting speed $v_l = 0.04$ m/s.
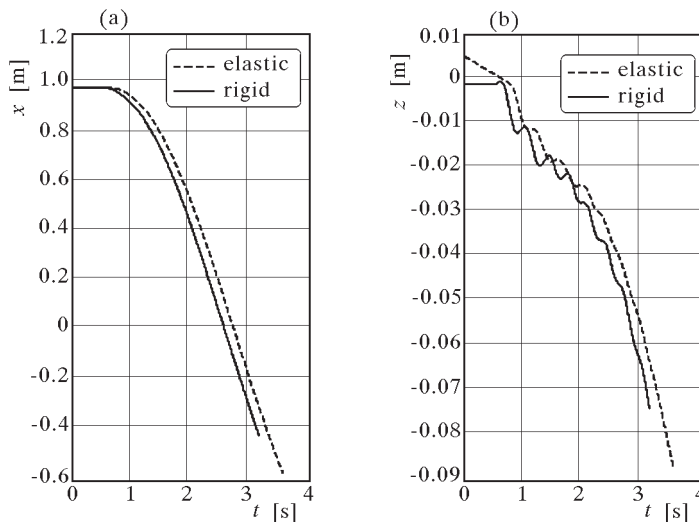
Fig. 5. Comparison of the results obtained for different models of the load – the displacements of the mass centre of the load (co-ordinates x and z)
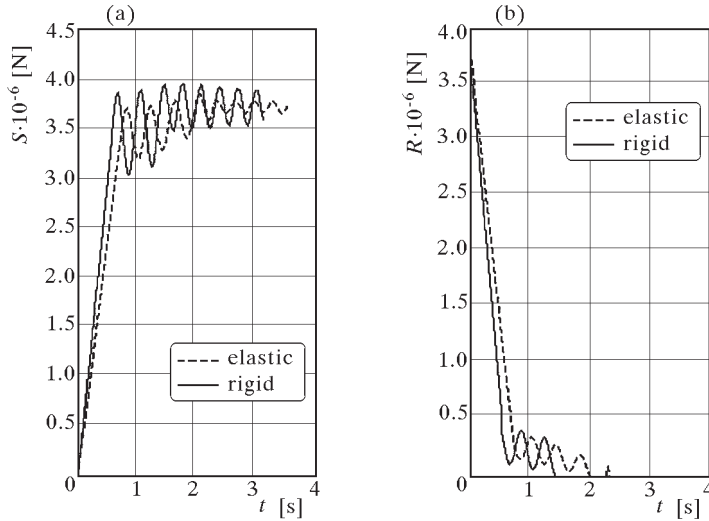
Fig. 6. Comparison of the results for different models of the load – the rope tension force S and the ground reaction force R

4.2. Calculation results for the model of a load placed on an elastic foundation

The calculations were carried out for the following data:

– container dimensions: $a = 2.5\,\text{m}$, $b = 6.0\,\text{m}$, $c = 2.5\,\text{m}$
– mean density of the container material $\rho = 850.0\,\text{kg/m}^3$
– properties of the foundation: coefficient of elasticity $k = 1.5 \cdot 10^7\,\text{N/m}$, coefficient of viscous damping $h = 2.0 \cdot 10^6\,\text{Ns/m}$
– properties of the rope: coefficient of elasticity $c_l = 1.4 \cdot 10^7\,\text{N/m}$, coefficient of viscous damping $b_l = 0.4 \cdot 10^6\,\text{Ns/m}$
– rope hoisting speed $v_l = 0.3\,\text{m/s}$.

Motion of the load (the analysed container was eccentrically loaded) is presented graphically in Fig. 7.

In Fig. 8 the time histories of friction forces in four points of the container – ground contact are shown. Differences in the time at which individual corners detach from the ground can be seen on these diagrams (the detachment of the corner from the ground is manifested by zero values of the normal force and the friction force at this point). It can be also observed that one of the corners (point F) impacts against the ground after detachment.

The directions along which the friction forces act and the trajectories of four corners of the load can be seen in Fig. 9.
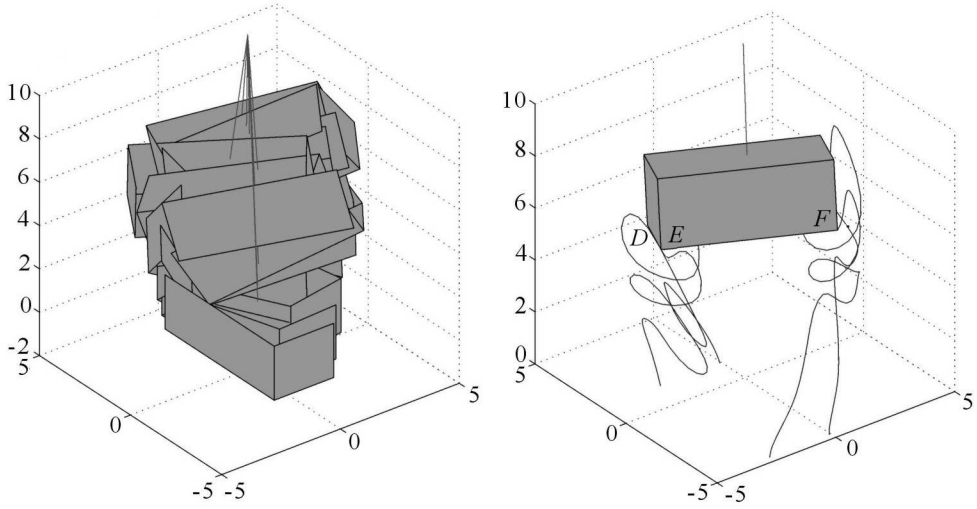
Fig. 7. Results of simulations of motion of the lifted container
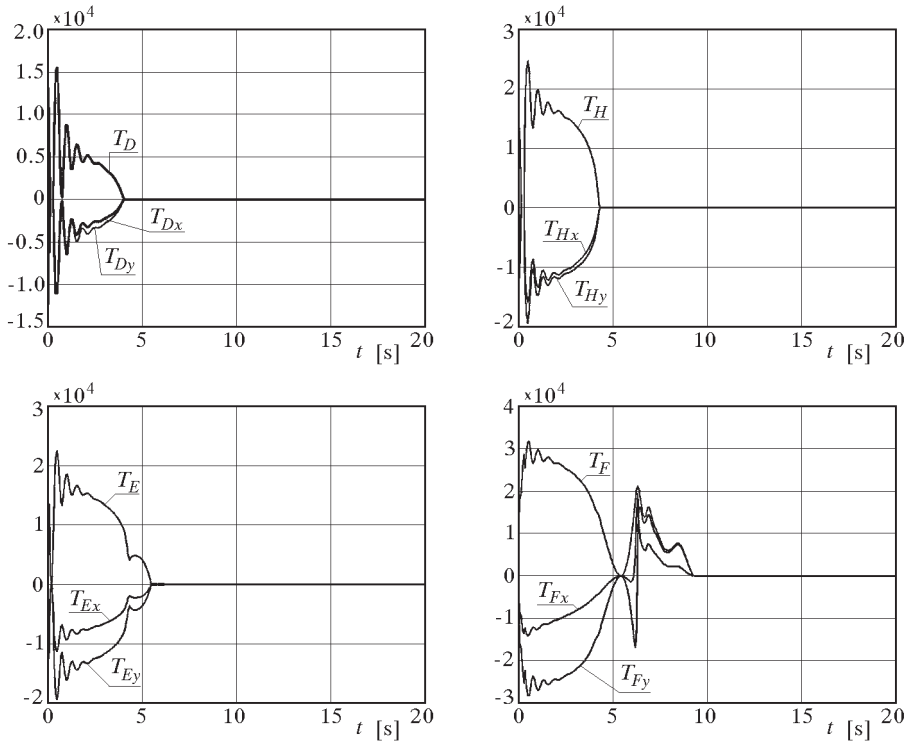
Fig. 8. Results of simulations of motion of the lifted container – values of the friction forces
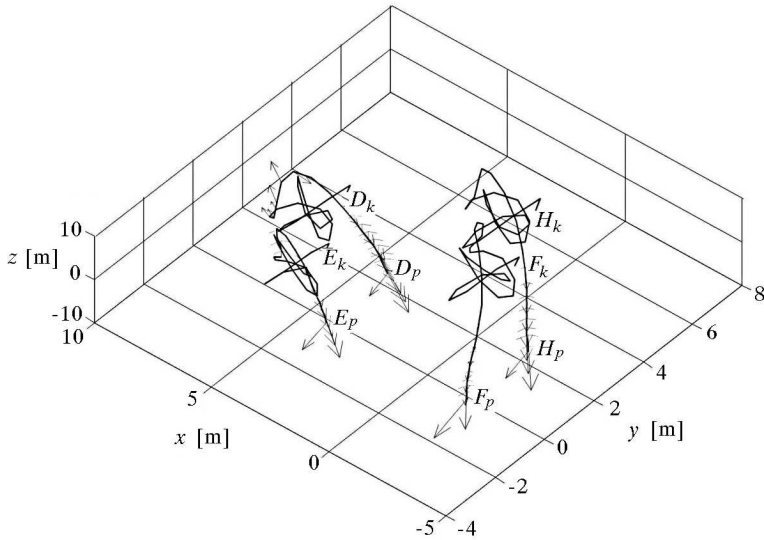
Fig. 9. Results of simulations of motion of the lifted container – directions of the friction forces
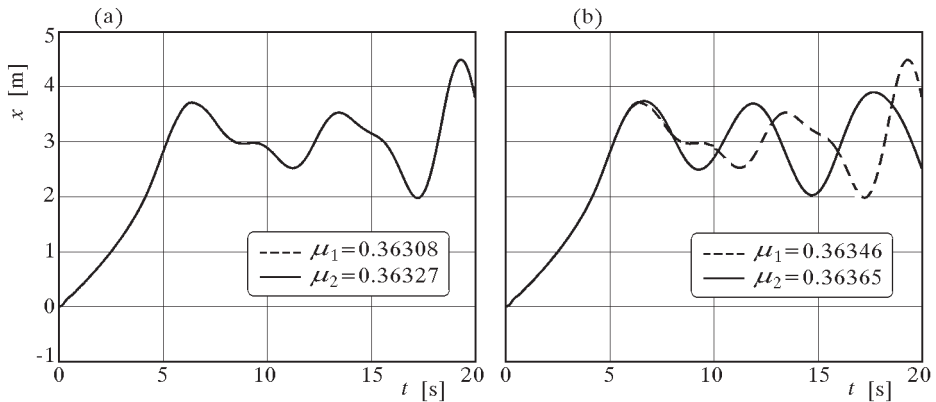
Fig. 10. Comparison of time histories of the co-ordinate x for various coefficients of friction

4.3.   Bifurcation of solutions

The calculations carried out for various parameters of the system revealed bifurcation of solutions that appeared during these calculations. For certain ranges of the parameters, a bifurcation of the solution takes place at a slight change in the value of one parameter. The results shown in Fig. 10b illustrate bifurcation of the solution that occurs at a slight change in the value of the coefficient of friction between the load and the foundation.

Figure 11 shows the time histories of the co-ordinates y and φ for different values of the coefficient of friction (within the range $0.363 \leqslant \mu \leqslant 0.365$). For the value $\mu \cong 0.3635$, a distinct change in the character of the time history of the solution occurs. The remaining co-ordinates behave in a similar way – the time histories of ϑ and ψ can be seen in Fig. 12.
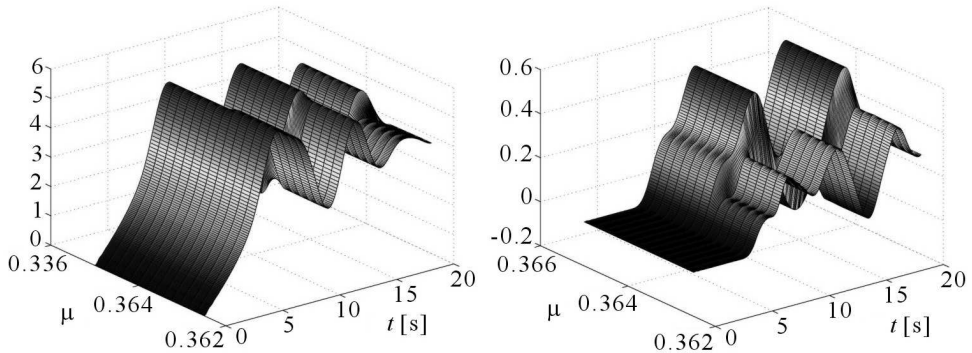
Fig. 11. Bifurcation of the solution (co-ordinates y and φ) resulting from a change in the coefficient of friction μ
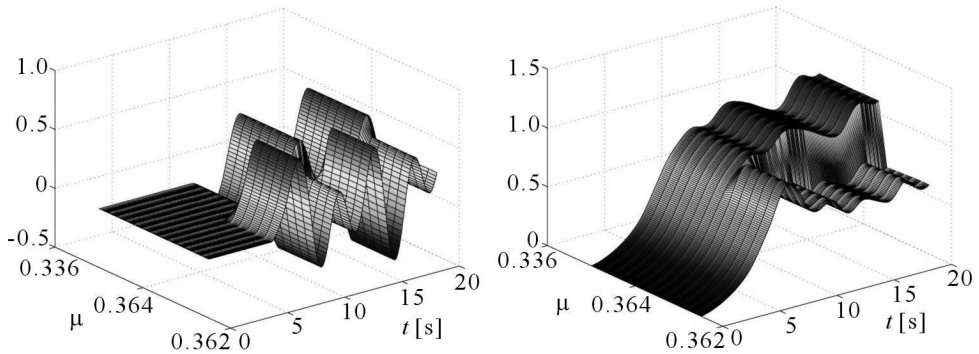
Fig. 12. Bifurcation of the solution (co-ordinates ϑ and ψ) resulting from a change in the coefficient of friction μ

4.4. Conclusions

For the three-dimensional model of the crane and the load in the form of a body, the algorithm that aims at the analysis of the load dynamics must take into account:

  – the rope and system tensioning during which the lifted load remains still

- the beginning of motion (it can be translation, rotation around the body edge, rotation around one of the corners)
- complete detachment of the lifted load from the foundation
- possibility of accidental impacts of the load against the ground
- general motion of the lifted load (including active or passive rope-affected constraints).

The global behaviour (motion) of the load contacting the ground can be described in such a way that the deformations of the load itself can be neglected.

The physical models of the load discussed in this study, it means: a rigid body located on a rigid foundation and a rigid body interacting with a foundation characterised by elastic and damping properties, proposed to be used in simulations of the lifting of the load from the ground, seem to be suitable for the purpose. The models used are accurate enough for the analysis of motion of the load.

The *Mathematica* package used in the above-mentioned calculations allows one to solve the task effectively, although it requires individual consideration of each phase of the lifting of the load from the ground. Its advantage lies in the possibility of obtaining many formulas in an analytical form.

The application of the *Matlab* package offers the possibility of numerical analysis of the whole lifting process, as well as of the transporting and lowering the lifted load, independent of the sequence of such phenomena as detachment, rotations, impacts, and sliding.

The calculations made for various values of the parameters of the model allowed for determination of the change in the character of the solution (solution bifurcation) in certain regions of the assumed values of these parameters.

References

1. Borkowski W., Konopka S., Prochowski L., 1996, *Dynamika Maszyn Roboczych*, WNT Warszawa

2. Grabski J., 1998, Analysis of engineering machine dynamics using matrix methods, *Scientific Bulletin of TUL*, **804** (in Polish)

3. Grabski J., Strzałko J., 1997, Automatic generation of Boltzmann symbols for mechanical problems, *Mechanics and Mechanical Engineering*, **1**, 1, 61-77

4. Hakala I., Sorsa T., 1998, Sway Prevention in RTG Cranes, *Koncranes'World* (http://www.kcinet.com/kciworld/spring1998)

5. Jedliński W., Grzesikiewicz W., 1990, Dynamics of working elements of engineering machines, including control, shown on the example of a telescopic crane, Reports of the Central Programme of Fundamental Investigations 02.05, Warsaw Technical University, Warsaw (in Polish)

6. Konderla P., 1993, A Contact problem approach for heterogeneous body by boundary element method, *XI Polish Conference on Computer Methods in Mechanics*, **1**, 441-448

7. Kurnik W., 1997, *Divergent and Oscillating Bifurcation*, WNT, Warsaw (in Polish)

8. Lee H.H., 1998, Modeling and control of a three-dimensional overhead crane, *ASME J. Dyn. Systems Meas. Control*, 120, 471-476

9. Maczyński A., Kościelny R., 1999, A dynamic model to optimisation working motions of a mobile crane, *Proc. Tenth World Congress on the Theory of Machines and Mechanisms*, Oulu, Finland

10. Miyata N. et al., 2001, Development of feedforward anti-sway control for highly efficient and safety crane operation, *Mitsubishi Heavy Industries, Ltd. Technical Review*, **38**, 2, 73-77

11. Strzałko J., 1998, Energy criterion of correctness of equations of motion and verification of their solutions in machine dynamics issues, *Scentific Bulletin of TUL*, **795** (in Polish)

12. Strzałko J., Grabski J., 1995, Dynamic analysis of a machine model with time-varying mass, *Acta Mechanica*, **112**, 173-186

13. Strzałko J., Grabski J., 1998, Computer simulation of the load lifting and transporting process, *XI Conference on Problems in Development in Engineering Machines*, 327-334 (in Polish)

14. Tomczyk J., Cink J., 1999, The optimisation of the flexibly suspended loads transport by microprocessor controlled overhead cranes, *Proc. Conference OPTI'99*, Orlando, Florida, USA

15. Wojnarowski J., Oziemski S., Nowak A., 1990, Modelling of reflection phenomenon during the bridge crane drive, Reports of the Central Programme of Fundamental Investigations 02.05, Warsaw Technical University, Warsaw (in Polish)

16. Wriggers P., Zavarise G., 1993, Recent trends in computational methods for contact problems, *XI Polish Conference on Computer Methods in Mechanics*, 127-148

Analiza dynamiki procesu podnoszenia ładunku

Streszczenie

W pracy zostały omówione propozycje modeli przeznaczonych do wykorzystania w analizie dynamiki ładunku podnoszonego przez dźwignice. Szczególna uwaga została zwrócona na zjawiska zachodzące przed oderwaniem ładunku od podłoża. Spośród dwóch przedstawionych modeli ładunku bardziej przydatny do analizy procesu podnoszenia okazał się model w postaci sztywnej bryły i sprężystego podłoża. Wyniki otrzymane z przeprowadzonych obliczeń numerycznych ujawniły zjawisko bifurkacji rozwiązania przy niewielkiej zmianie wartości parametrów modelu.